

Predicting compressive strength of cement-stabilized earth blocks using machine learning models incorporating cement content, ultrasonic pulse velocity, and electrical resistivity

Navaratnarajah Sathiparan & Pratheeba Jeyanathan

To cite this article: Navaratnarajah Sathiparan & Pratheeba Jeyanathan (24 Jul 2023): Predicting compressive strength of cement-stabilized earth blocks using machine learning models incorporating cement content, ultrasonic pulse velocity, and electrical resistivity, Nondestructive Testing and Evaluation, DOI: [10.1080/10589759.2023.2240940](https://doi.org/10.1080/10589759.2023.2240940)

To link to this article: <https://doi.org/10.1080/10589759.2023.2240940>



Published online: 24 Jul 2023.



Submit your article to this journal [↗](#)



Article views: 120



View related articles [↗](#)




View Crossmark data [↗](#)



Citing articles: 1 View citing articles [↗](#)



Predicting compressive strength of cement-stabilized earth blocks using machine learning models incorporating cement content, ultrasonic pulse velocity, and electrical resistivity

Navaratnarajah Sathiparan^a and Pratheeba Jeyanathan^b 

^aDepartment of Civil Engineering, Faculty of Engineering, University of Jaffna, Kilinochchi, Sri Lanka;

^bDepartment of Computer Engineering, Faculty of Engineering, University of Jaffna, Kilinochchi, Sri Lanka

ABSTRACT

The quality monitoring technique for Cement stabilised earth blocks (CSEBs) is so challenging that it is often neglected. This study has investigated the possibility of using machine learning to predict the compressive strength of CSEBs based on cement content, electrical resistivity and Ultrasonic pulse velocity (UPV) as a potential way to enhance quality control. The study considered three types of soil and different cement content in the preparation of CSEBs with 10 different cement-soil mixtures. Various machine learning models were proposed to predict the compressive strength of CSEBs. The models were evaluated using 180 experimental datasets, and the best model for predicting the compressive strength of CSEBs was selected. The ANN and BTR models performed better than the other machine learning models tested in this study for predicting the compressive strength of CSEBs. The results show that a combination of cement content, electrical resistivity and UPV can be used to assess the quality of CSEBs more accurately, which can contribute to the knowledge base and be applied in the real world. Materials scientists and engineers can use reliable predictive models to assess the strength properties of both new and old brick structures without damage or loss of use.

ARTICLE HISTORY

Received 5 June 2023

Accepted 21 July 2023

KEYWORDS

CSEB; compressive strength; UPV; electrical resistivity; machine learning

Introduction

Masonry blocks are a crucial element of the construction industry, providing a strong and reliable foundation for walls and other structures. Although fired clay brick and concrete blocks are mostly used as masonry units for house construction, they are environmentally unfriendly materials. The preparation of raw materials and production of these materials has high energy embodied and CO₂ emissions [1]. In recent years, cement-stabilised earth blocks (CSEBs) have become an alternative option for masonry house construction due to their favourable aspects such as being economical, environmentally friendly, and providing better thermal comfort [2,3]. However, their mechanical characteristics are significantly affected by the characteristics of the soils used for their production. Also, they are widely used in rural areas where masonry unit production and house construction are done by homeowners themselves [4]. The

production of CSEBs requires careful consideration of a variety of factors beyond just the cement content. In addition to controlling the cement content, it is essential to carefully select the soil, manufacture the blocks properly, and construct the house with attention to detail. While there are many recommendations for suitable soil types and production procedures, few focus on assessing the quality of CSEBs [5]. The best way to ensure quality is through lab testing, but access, cost, and time can be significant challenges, especially in rural areas. Therefore, it is crucial to prioritise quality control measures at every stage of the process to ensure safe and sustainable housing construction.

In general, the measurement and estimation of the compressive strength of CSEBs is based on experimental testing, mathematical modelling and machine learning models. Experimental testing is a useful system as it produces results that can be replicated. However, it must be tightly controlled to be useful. It can also be easily influenced by internal or external factors that can change the results obtained. Mathematical equations can provide a quick and easy way of predicting compressive strength. However, they are only as good as the data used to generate them. If the data is not representative of actual conditions, the predictions may not be accurate. Machine learning models can provide accurate compressive strength predictions. They can also learn from new data and improve their predictions over time. However, they require large amounts of data to train and can be difficult to interpret.

There are several methods for testing the compressive strength of earth blocks, varying specimen size, loading rate and destructive or non-destructive testing. The cube specimen, the half-block stacked specimen and the full-size block specimen are used to measure the compressive strength of CSEBs. In addition to common laboratory tests such as the uniaxial compression load test, some pioneering work has recently been published on the use of mildly destructive or non-destructive techniques. For destructive techniques, Lombillo et al [6] used the flat-jack, hole-drilling and mini-pressure-metre techniques to assess the stiffness and deformation of rammed earth in situ. All of the above studies used destructive testing, which involved testing a large number of blocks and consuming more energy, time and material. It may therefore be uneconomical [7].

As such, predicting the compressive strength (f_c) of CSEBs is a significant aspect of ensuring the quality of any building project. Non-destructive testing (NDT) provides an effective alternative option for predicting the f_c of masonry. NDT is a testing technique that has the potential to measure material properties without damaging the sample being tested. These methods consist of X-ray testing, infrared thermography, acoustic emission testing, and ultrasonic testing [8,9]. NDT can be used to measure a variety of characteristics such as compressive strength, tensile strength, elastic modulus, and thermal properties [10,11]. The use of NDT to predict the f_c of masonry has numerous advantages. For example, it eliminates the need for expensive and time-consuming destructive testing and can be used on both new and existing structures. Additionally, NDT can provide a precise measurement of the f_c of construction material, which is closer to traditional destructive testing methods [12]. This is because NDT can measure a material's compressive strength from a variety of angles, allowing for a more comprehensive assessment of the material's strength.

Several non-destructive test methods can estimate the quality of construction materials [13,14]. Some of these methods, such as rebound hammer, ER and UPV are widely

used for concrete because they are simple and easy [15–18]. However, most of the research on these methods focused on cement mortar and concrete. But the quality assessment of CSEBs based on NDT is limited.

Ksinikota and Tripura [19] developed an empirical formula to predict the fc of hollow compressed stabilised earth blocks using UPV measurement. The authors used five different cement content and a single soil type for the casting of blocks. They developed an empirical formula between UPV (in km/s) and compressive strength (in MPa) of blocks as shown in Equation (1)–(3) for different moisture conditions such as air dry, oven dry and wet conditions, respectively. The proposed equation shows a strong correlation between predicted and experimental fc for all moisture conditions ($R^2 > 0.95$).

$$fc - air\ dry = 3.924UPV - 2.882 \quad (1)$$

$$fc - oven\ dry = 6.349UPV - 5.086 \quad (2)$$

$$fc - wet = 2.888UPV - 2.667 \quad (3)$$

Sathiparan et al. [5] reported the correlation between ER, UPV and fc of CSEBs. Compared with individual correlation, the empirical model developed using both NDT measurements improves in correlation among the measured and predicted fc of CSEBs. They proposed an empirical formula between ER (in $k\Omega.cm$), UPV (in km/s) and fc (in MPa) as shown in Equation (4) and (5) for air-dry and wet conditions, respectively. The proposed equation expressed a solid correlation among experimental and predicted fc for air dry and wet conditions as R^2 equal 0.93 and 0.90, respectively.

$$fc - air\ dry = 0.766 \times 2.390^{UPV} \times E^{-0.007} \quad (4)$$

$$fc - wet = 0.548 \times UPV^{2.119} \times E^{-0.150} \quad (5)$$

Machine learning (ML) algorithms have become common for predicting the characteristics of building materials [20–22]. Machine learning is the most effective method for predicting the properties of construction materials, which depend on many variables [23,24]. Moreover, various machine learning (ML) techniques, such as linear regression (LR), decision tree regression (DTR), random forest regression (RFR), support vector regression (SVR), K-nearest neighbours (KNN), bagging regression (BGR), and others, have been used to predict the compressive strength of building materials [25–27]. Several studies have used non-destructive testing (NDT) measurements and machine learning (ML) techniques to predict the properties of rock [28,29], concrete [30–33] and timber [34]. However, there is little research on predicting the compressive strength (fc) of CSEBs using NDT measurements and ML techniques.

Therefore, the present study aims to forecast the fc of CSEBs by using two NDT measurements (ER and UPV) through ML techniques, to assess the quality of the CSEBs without causing damage. The CSEBs were made with ten different combinations of cement-to-soil ratios and soil types. Based on the results, the study examined the correlations between the cement content, UPV, ER, and fc (dry and wet) of CSEBs by using various ML techniques.

Experimental program

Materials used

Ordinary Portland cement (OPC) was used as a binder. Three different lateritic soil types, designated as soils 1, 2, and 3, were selected for the study from university premises in Kilinochchi, Sri Lanka. The soil was cleaned of impurities including leaves and tree roots. They were passed through 10 mm sieves before being utilised for the experiment. Figure 1 displays the physical appearance of the soils.

Figure 2(a,b) illustrate the particle-size distribution of the soils and the correlation between dry density and moisture content for each soil type. Soil 3 had the lowest MDD of the three soil types. The highest dry densities were attained by soil 2.

Table 1 lists the physical parameters, results of the Proctor compaction test, particle size traits, and Atterberg limit for soils as well as the chemical composition of cement and soils. While soil 2 was lighter, soil 1 was denser. Soil 1 has a high amount of gravel (18.9%), and soil 2 has more fines (4.5%). All soils were found to have SiO_2 , which is the most common oxide, followed by Fe_2O_3 . Another important aspect of the soils' chemical makeup is their low concentrations of Na_2O and K_2O , except for soil 3, which has 0.78% K_2O .

Mix design

The research aimed to predict the f_c of CSEBs using NDT measurements. The mortar had different mechanical properties and was made from 10 mixtures of varying types of soil and cement content. The experiment used four cement contents (8%, 12%, 16%, and 20% of soil volume) to make the mortar. Table 2 shows the soil and cement amounts for a one-metre cube mix. The water volume for mixing the cement and soil was another vital variable. Excessive water would make the mortar weak, while too little water would make it stiff and dry. A constant W/C ratio or fixed slump was preferred for consistent workability [35]. The study used different types of soil and cement content, so

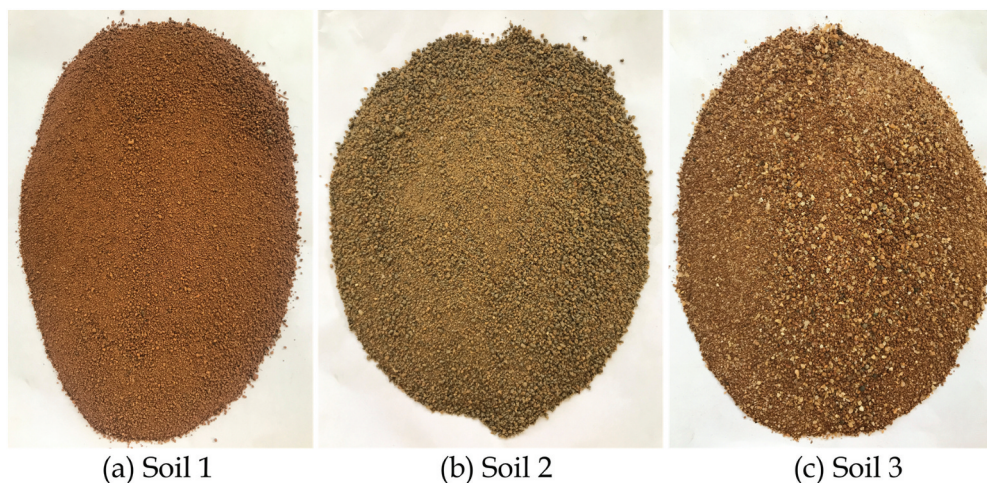


Figure 1. The physical appearance of soils used in the experimental program.

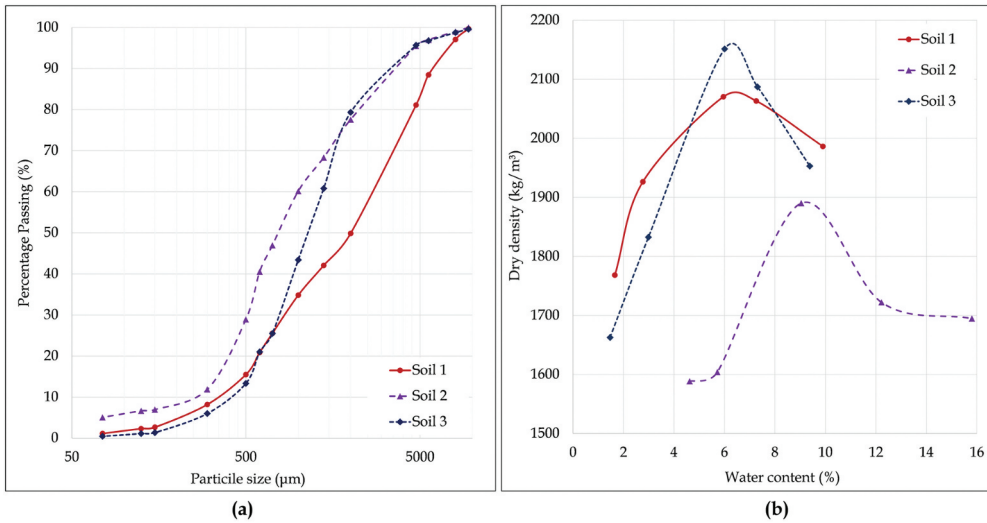


Figure 2. Soil characteristics (a) particle size distribution and (b) test results of proctor compaction.

Table 1. Cement and soil characteristics.

Characteristics	Properties	Cement	Soil 1	Soil 2	Soil 3
Physical properties	Bulk density (kg/m ³)	1280	1168	1258	1456
	Specific density	3.15	2.50	2.35	2.55
Proctor test	Optimum moisture content, OMC (%)		6.5	9.2	6.5
	Maximum dry density, MDD (kg/m ³)		2080	1895	2160
Grain size	Gravel (%)		18.9	4.5	4.3
	Sand (%)		80.0	90.4	95.2
	Silt & clay (%)		1.1	5.1	0.4
Atterberg limit	Liquid limit, WL (%)		31.0	27.0	20.8
	Plastic limit, PL (%)		21.5	19.4	18.5
	Plasticity index, IP (%)		9.5	7.6	2.3
Chemical composition (% wt.)	CaO	66.55	0.03	1.13	0.60
	SiO ₂	20.60	76.49	74.23	80.40
	Al ₂ O ₃	4.51	2.49	3.79	2.46
	Fe ₂ O ₃	3.62	4.89	6.49	4.14
	MgO	1.17	0.46	0.44	0.19
	Na ₂ O	0.40	0.22	0.16	1.30
	K ₂ O	0.39	0.21	0.27	0.78

Table 2. Materials requirement for 1 m³ mortar mixture.

Mix	Cement (kg)	Soil 1 (kg)	Soil 2 (kg)	Soil 3 (kg)	Water (l)
S1-08	148.9	1697.9			240.1
S1-12	215.3	1637.3			288.9
S1-16	277.2	1580.8			334.3
S1-20	334.9	1528.1			376.8
S2-08	148.9		1828.8		290.2
S2-12	215.3		1763.4		337.2
S2-16	277.2		1763.4		337.2
S3-08	148.9			2116.6	240.1
S3-12	215.3			2041.0	288.9
S3-16	277.2			970.6	334.4

a specific W/C ratio was required for a uniform mixture [36]. The W/C ratio was based on the optimal moisture content for the MDD and the cement amount in the mix.

Initially, the cement and soil were dry-mixed thoroughly and water was added and mixed well again. The wet mix was transferred into wooden moulds of 100 mm by 100 mm by 100 mm, and the mix was manually compressed with 25 strokes of a steel rod for each of the three layers. After one day, cube samples were removed from the moulds and cured. They were stored in a lab environment for 28 days at room temperature (27–33°C) for curing. Nine cubes were used to measure each mix's density and compressive strength.

Testing

Ultrasonic pulse velocity

A portable ultrasonic NDT digital indication tester was utilised to measure the ultrasonic pulse velocity of CSEBs following the American Society for Testing Materials (ASTM) C597 [37]. The ultrasonic pulse analyser, PULSONIC model 58-E0046/5, is used to measure the velocity of the ultrasonic pulses through the mortar cubes. The equipment's configuration is shown in Figure 3(a). A portable device that measures the speed of ultrasound pulses in materials with a transit time range of 16 ms, a 2 MHz sampling rate, a resolution of 0.1 s, and a transmitter output of 1200 V. The data analysis was based on the average value from three measurements taken along two horizontal and one vertical direction. In this study, a frequency of 54 kHz was used for UPV measurements, as it is more suitable for evaluating block properties [38]. The instrument was calibrated using a reference bar (25.4 μ s) before the start of the test. Vaseline was used as a couplant to ensure better contact between the block surface and the transducer. The transducers were positioned firmly against the two opposite block surfaces until a stable transit time was displayed. The distance travelled by the ultrasound wave and the pulse transit time were recorded. UPV measurements were taken in three directions, one in the direction of compaction and the other two perpendicular to the direction of compaction, and their average is expressed as UPV. A total of 180 blocks were subjected to ultrasonic testing and the same were used for mechanical testing. The impulse velocity was calculated using Equation (6).

$$UPV = L/T \quad (6)$$

where, UPV = ultrasonic pulse velocity (km/s), L = distance travelled by the pulse (km) and T = transit time (s).

Electric resistivity

A non-destructive test equipment was utilised to measure the ER of CSEBs following the ASTM C1876 [39] standard. Resipod concrete resistivity metre (38 mm probe spacing) model HM-952 is used for measuring the ER of the surface of mortar cubes. It can measure the surface resistivity from 1 to 1000 k Ω cm [40]. The equipment's configuration is shown in Figure 3(b). The average value from four readings taken on the two sides, the bottom, and the top surfaces was used for analysis.



Figure 3. Testing setup (a) UPV, (b) ER, and (c) compression.

Compression test

The compression test was carried out using a Universal Testing Machine (UTM) by displacement control method as per ASTM C109 [41]. Cubes of $100 \times 100 \times 100 \text{ mm}^3$ were used for the test. The cubes were air-dried for 28 days at room temperature and then tested for dry f_c . To measure the saturated f_c , the cubes were soaked in water for one day after 27 days of air-drying and then tested with a 2 mm/min axial load. The test setup is illustrated in Figure 3(c).

Machine learning modelling

ML modelling flow

Figure 4 presents the outline of the ML modelling flow chart. A total of 180 data (90 for dry conditions and 90 for wet conditions) were gathered from the experimental program to create a valid model for predicting the compressive strength of CSEBs. Linear regression (LR), artificial neural network (ANN), boosted tree regression (BTR), random forest regression (RFR), K-nearest neighbours regression (KNN),

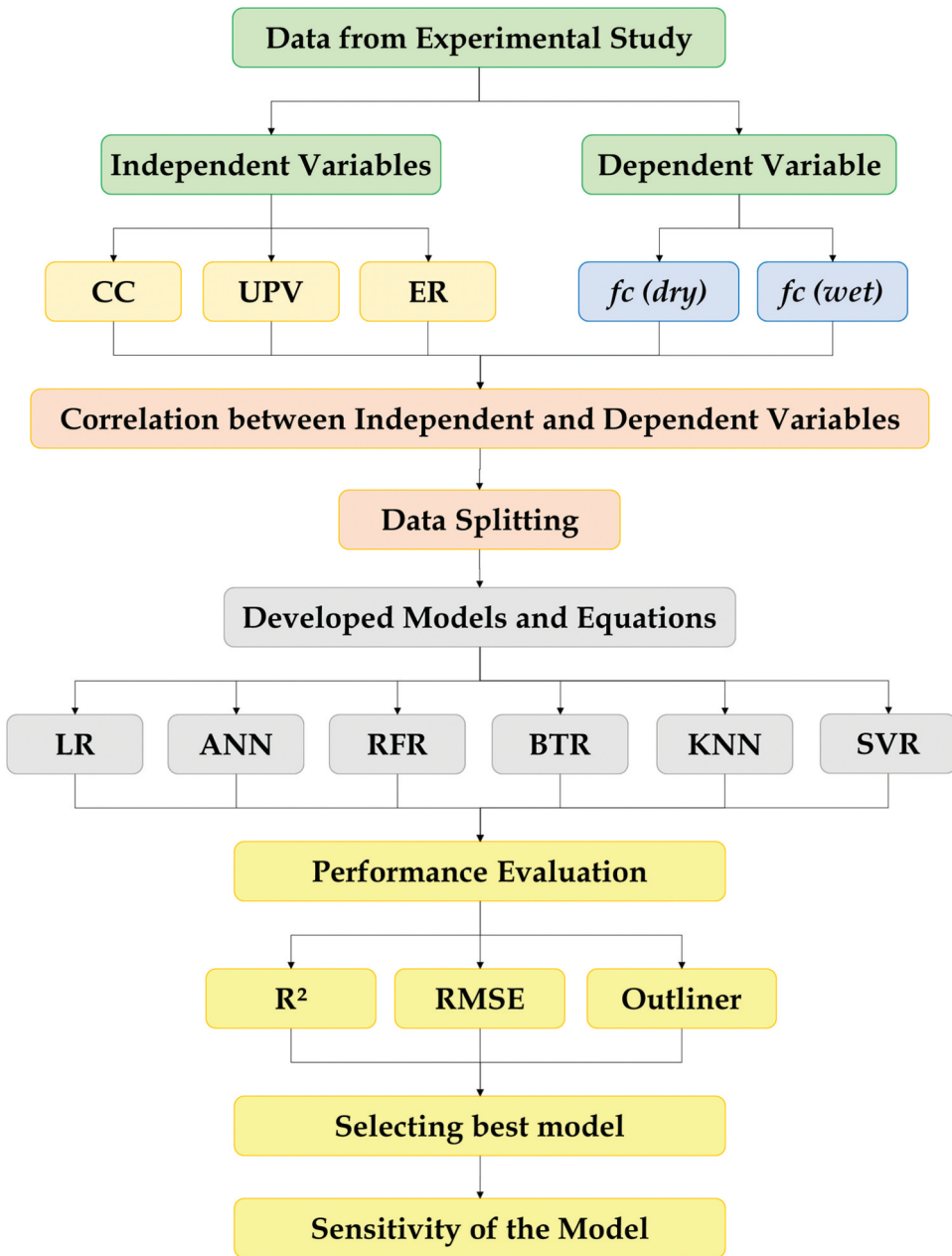


Figure 4. Working flow chart for machine learning modelling and analysis.

and support vector regression (SVR) are the six algorithms used to predict the compressive strength of CSEBs. Although deep learning-based models may provide more accurate predictions, due to limited data and the possibility of overfitting, the ML models are limited to conventional techniques. It should also be noted that even conventional models such as ANN, BDT and RFR provide accurate predictions for the data used in this study. The following performance indicators were applied: coefficient

of determination (R^2), root mean squared error (RMSE), and outlier for the accuracy of the models.

Machine learning technique

Linear Regression (LR)

The LR model, as specified in Equation (7), is the usual method for predicting the compressive strength of CSEBs [42].

$$f_c = a + b(CC) + c(UPV) + d(ER) \quad (7)$$

where f_c in MPa, CC in weight fraction, UPV in km/s and ER in $k\Omega.cm$. a , b , c and d are model constants.

Artificial Neural Network (ANN)

ANN is an ML tool that can analyse and compute data in a similar way to the human brain. It is an ML method that is often used in construction engineering to predict the future outcomes of different numerical problems. An ANN model has three main layers: input, hidden, and output layers [43,44]. The output layer has the compressive strength of CSEB, and the input layer has cement content, UPV, and ER. The hidden layer usually has more than two levels. The input and output layers depend on the data and the goal of the model, while the hidden layer depends on the weight, transfer function, and bias of each layer to other layers [45,46]. There is no fixed way to design a network structure. So, the number of hidden layers and neurons is found by optimising the parameters. The best number of iterations is the one that meets the key criteria of the network's training process: the highest R-value and lowest root mean square error (RMSE).

Random Forest Regression (RFR)

Random Forest (RF) Regression is an ensemble learning algorithm that combines the outputs of many regression decision trees. Each tree is built with a random vector that is chosen from the input variables and has a uniform distribution in the forest [47]. The method uses bootstrap aggregation and random feature selection to average the predictions of the forest [48].

Boosted Tree Regression (BTR)

BTR is a method that uses multiple regression trees to make predictions. A regression tree is a model that splits the input data into smaller groups based on some criteria and then assigns a constant value to each group. Boosting is a technique that improves the accuracy of the model by combining many simple trees into one complex tree [49]. Boosting works by fitting a new tree to the errors of the previous tree and then adding them together to get a better prediction [50]. BTR can handle different types of data, nonlinear relationships, and interactions between variables [51].

K-nearest Neighbors (KNN)

KNN is a supervised learning algorithm that can be used for classification or regression problems. It works by finding the (in the present study $k = 5$) closest training examples to a new data point and assigning it a label or a value based on the majority vote or the average of its neighbours [52]. KNN is a non-parametric method, meaning that it does not make any assumptions about the underlying distribution of the data [53]. KNN is also a lazy learning method, meaning that it does not have a training stage, but rather stores all the training data and performs computation only when a prediction is needed [54]. KNN is simple and effective, but it can also be inefficient and sensitive to noise and irrelevant features [55].

Support vector machines

Support Vector Machines (SVMs) are supervised learning models that can be used for classification or regression problems. They work by finding a hyperplane that separates the data into different classes or predicts the value of a continuous variable [56]. SVMs are based on the idea of maximising the margin between the data points and the hyperplane, which makes them robust and effective in high-dimensional spaces [57]. SVMs can also use different kernel functions to perform non-linear classification or regression by mapping the data into higher dimensional feature spaces [58]. SVMs are versatile, memory efficient, and have strong theoretical foundations, but they also have some disadvantages, such as being sensitive to noise and outliers, requiring the careful choice of parameters and kernels, and not providing probability estimates [59].

Performance indicator

To evaluate the performance of the predicted models, Coefficient of determination (R^2) and Root Mean Squared Error (RMSE) were used, which are defined as Equation (8) and (9).

$$R^2 = 1 - \frac{\sum_{i=1}^n (P_i - E_i)^2}{\sum_{i=1}^n (E_i - \bar{E})^2} \quad (8)$$

$$RMSE = \sqrt{\frac{\sum_{i=1}^n (P_i - E_i)^2}{n}} \quad (9)$$

where, E_i and P_i are the measured and predicted values, respectively; \bar{E} is the mean of measured values; n is the number of the data used.

In addition, the outlier (OL) percentage is also considered a performance indicator by considering the predicted values are outside the 20% error line. The OL % was calculated by Equation (10).

$$OL = \frac{n_{OL}}{n} \times 100 \quad (10)$$

where, n_{OL} is the number of points outside the 20% error line and n is the total amount of data.

Cross-validation

K-fold cross-validation is a method for validating multi-class classification models. It randomly divides the dataset into several groups and uses one group for testing and the rest for training. In this study, fivefold cross-validation ($k = 5$) was used to evaluate the results. The data set was shuffled and divided into five groups. Each group was used once as the test set, while the other four groups were used as the training set. This procedure was repeated for all five groups. The average of the five test scores, together with the variance, is used as an estimate of the model's performance.

Experimental results

Figure 5(a,d) illustrate the UPV of CSEBs under dry and wet conditions, which can be influenced by various aspects such as cement content and aggregate type, aggregate dimension, W/C ratio, transducer spacing, curing age and moisture content [60]. The UPV increased with higher cement concentration. Among the soil types, soil 3 had the highest UPV for a given cement concentration, while soil 2 had the lowest. The greater amount of hydration products resulting from higher cement content filled more voids and increased the flexibility of the CSEBs, resulting in faster transmission of ultrasonic pulses through them. Soil 2 had a lower UPV value than the other two soil types due to inadequate block packing, resulting in reduced density. The study also showed that CSEBs saturated with water had a higher UPV. The moisture content of CSEBs has a significant effect on UPV. Research suggests that the UPV of mortar increases with increasing water content, as reducing the amount of air space in the ingredients can increase the UPV [61]. When saturated, water fills the voids in the mortar mix, resulting in faster wave motion.

The ER of CSEBs in dry and wet conditions is shown in Figures 5(b,e). According to recent studies [62], the ER of CSEBs is affected by several variables such as cement content, aggregate type and dimension, W/C ratio, curing age, moisture content and porous characteristics. The test results indicate that an increase in cement concentration leads to an increase in electrical resistance due to the cement hydration process. More cement in the mix produces more calcium silicate hydrate, which fills the pore spaces and creates a denser structure. The hydration process and subsequent free water consumption further increase the pore tortuosity for electric current, resulting in an increase in soil resistivity [62,63]. In addition, mortar with soil 3 had a higher ER value for specific cement content, while mortar with soil 2 had a lower ER value. The study also found that the degree of saturation had a significant effect on the resistivity of the soil block [64]. In general, wet CSEBs had lower ER due to the presence of water, which is an excellent conductor of electricity. As a result, the ER of the mortar decreased as its water content increased [62].

Figure 5(c,e) show the f_c of the CSEBs in dry and wet conditions. As the amount of cement in the mortar increased, so did their f_c . Mortar from soil 3 showed superior strength for a given cement concentration, whereas mortar from soil 2 showed lower strength due to weak bonding between the cement paste and the aggregates caused by its higher clay and silt content. The cement-colloidal structure showed much lower strength than the cement-granular matrix, although

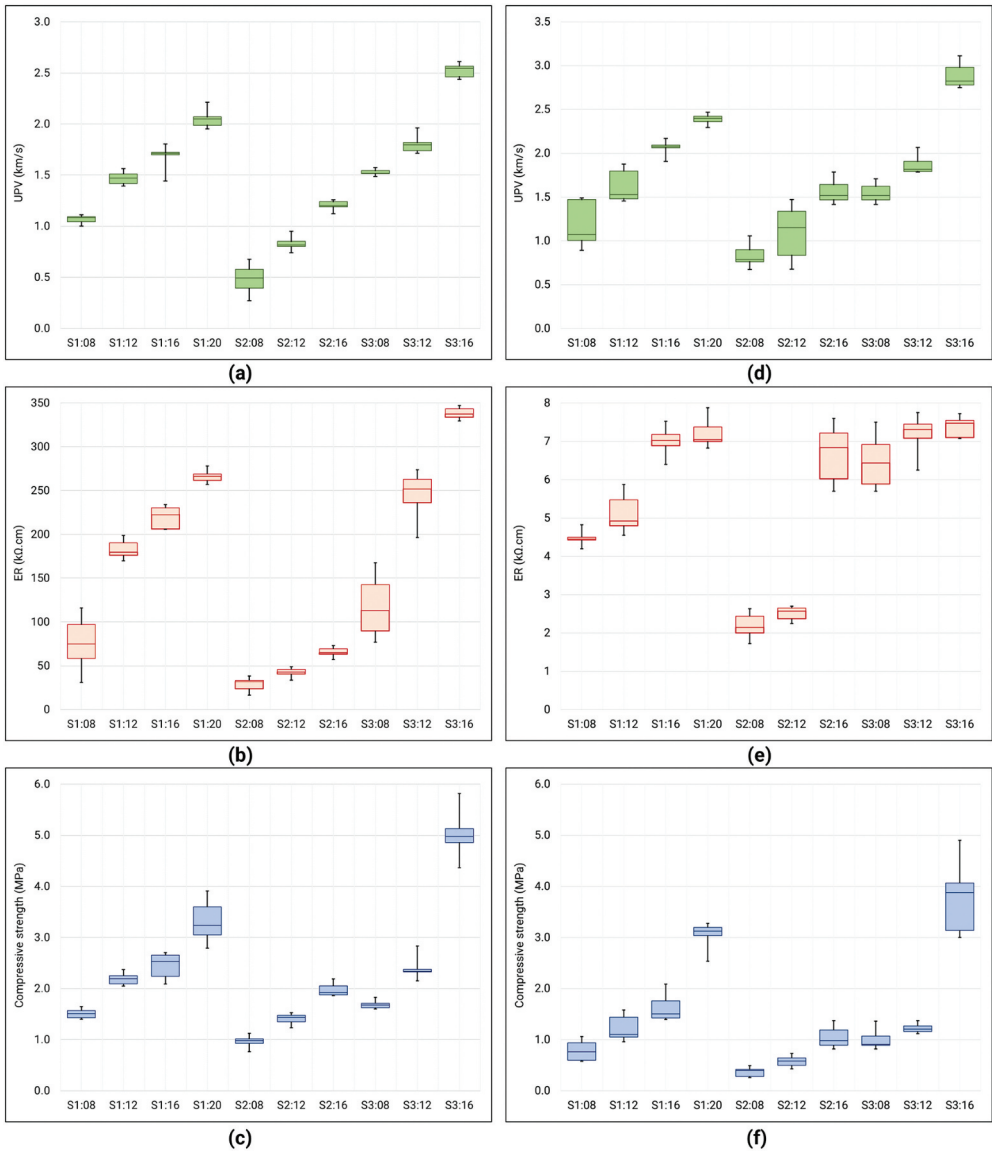


Figure 5. (a) UPV, (b) ER, (c) compressive strength for the specimen in dry condition and (d) UPV, (e) ER, (f) compressive strength for the specimen in wet condition.

the clay or silt minerals react with the cement and tend to become stable. The increased sand concentration of soil 3 had a beneficial effect on the f_c of CSEBs, while cohesive soil aggregates formed during mixing reduced the effectiveness of the cement. Due to the increase in pore water pressure and the liquefaction of unstable clay in the mortar matrix, the wet f_c was found to be lower than the corresponding dry f_c in all scenarios. This can be attributed to the instability caused by the above factors.

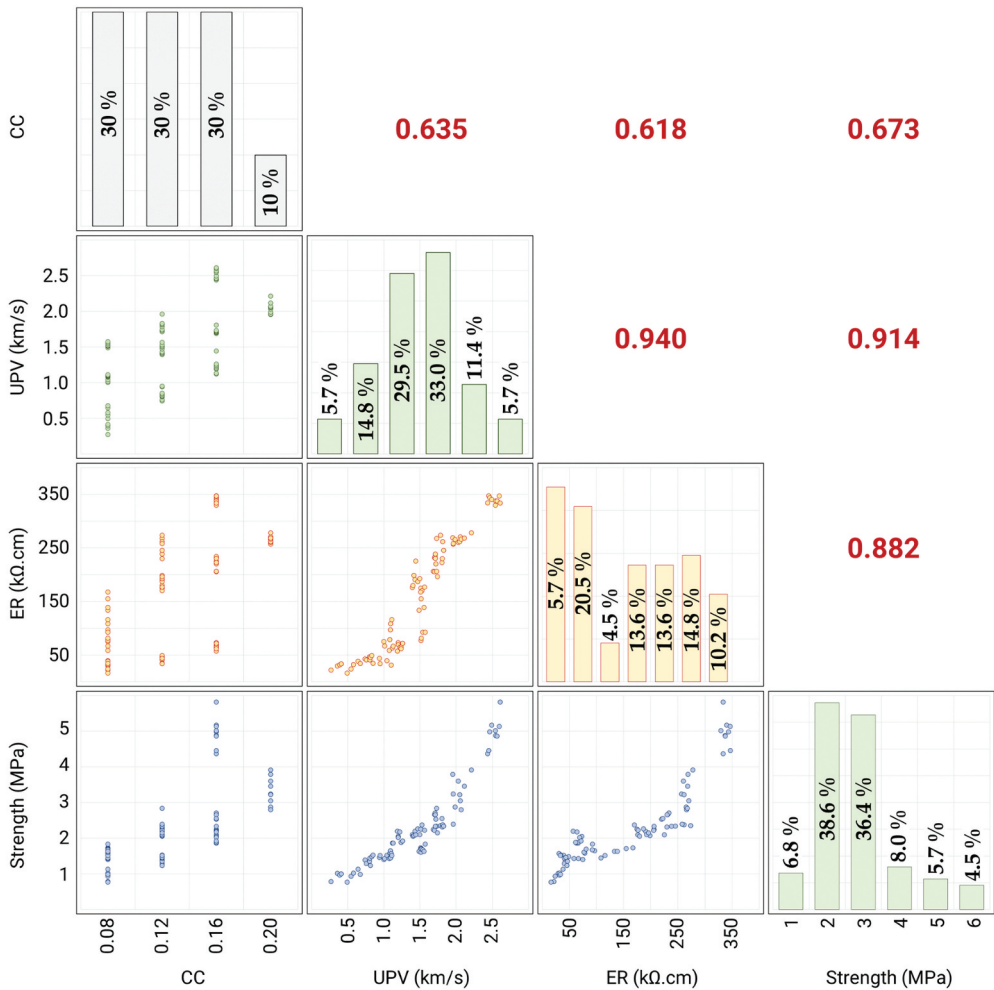


Figure 6. Correlation among independent and dependent variables in dry condition.

Statistical analysis

The input variables for this study were cement content, UPV and ER, while the output variables were f_c (dry) and f_c (wet). Figure 6 shows the descriptive statistics for the input and output data. It shows that the cement content varied between 0.08 and 0.20. For dry conditions the UPV varied from 0.27 to 2.61 km/s, the ER varied from 16.4 to 347.0 kΩ.cm and the f_c varied from 0.77 to 5.82 MPa. For wet conditions, UPV varied from 0.67 to 3.11 km/s, ER varied from 1.7 to 7.8 kΩ.cm and f_c varied from 0.26 to 4.90 MPa.

The study presents a comprehensive set of experimental data and statistical analysis was performed to assess the correlation between the variables mentioned. The results indicate that there is a significant correlation between UPV and ER, as shown in Figure 7 using Pearson's correlation. Furthermore, the relationship between UPV, ER and f_c was found to be much stronger. In particular, the metrics for dry conditions showed a more significant correlation than for wet conditions.

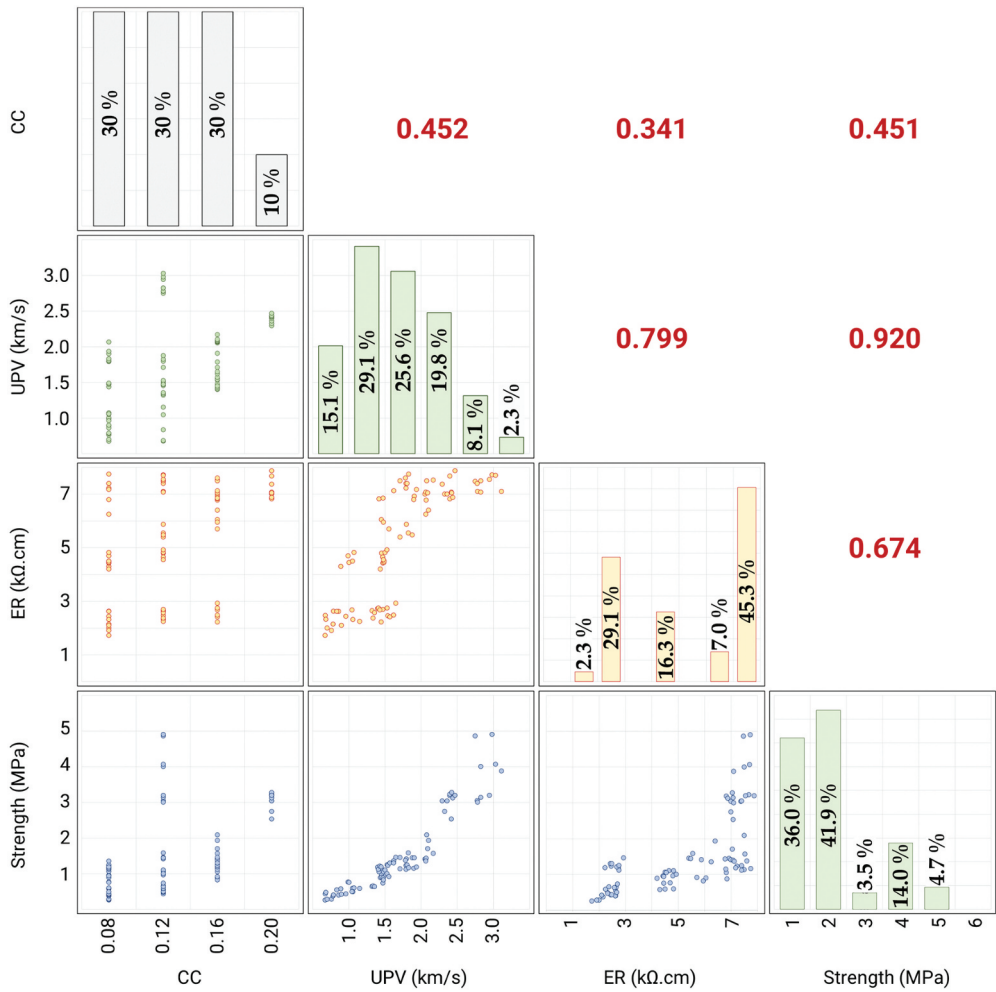


Figure 7. Correlation among independent and dependent variables in wet condition.

Table 3. Three-way ANOVA analysis for experimental results.

	Source	Type III Sum of Squares	df	Mean Square	F	Sig.	Contribution (%)
<i>f_c</i> (dry)	CC	53.32	3.00	17.77	25.99	5.48E-12	16.1
	UPV	109.62	71.00	1.54	21.35	1.35E-08	13.2
	ER	11.76	86.00	1.29	114.48	0.07	70.7
<i>f_c</i> (wet)	CC	39.83	3.00	13.28	17.39	7.89E-09	35.7
	UPV	101.51	67.00	1.52	29.73	1.13E-10	61.0
	ER	87.91	67.00	1.31	1.63	0.12	3.3

Table 3 shows the full range of experimental data, indicating that ER had a greater effect on *f_c* in dry conditions, while UPV had a more significant effect on *f_c* in wet conditions. However, ER had no significant effect on *f_c* in wet conditions.

Table 4. Performance indicator for each ML techniques.

Condition	ML technique	Train		Test		Total		OL
		R ²	RMSE	R ²	RMSE	R ²	RMSE	
Dry	LR	0.854 ± 0.009	0.428 ± 0.012	0.811 ± 0.061	0.454 ± 0.044	0.845	0.433	31.8
	ANN	0.964 ± 0.013	0.211 ± 0.044	0.970 ± 0.013	0.180 ± 0.046	0.965	0.205	1.2
	RFR	0.950 ± 0.020	0.243 ± 0.039	0.940 ± 0.035	0.246 ± 0.049	0.948	0.244	2.3
	BTR	0.982 ± 0.004	0.151 ± 0.012	0.936 ± 0.042	0.251 ± 0.048	0.973	0.171	2.3
	KNN	0.952 ± 0.008	0.245 ± 0.023	0.957 ± 0.028	0.207 ± 0.051	0.953	0.237	4.5
	SVM	0.966 ± 0.009	0.203 ± 0.025	0.949 ± 0.028	0.228 ± 0.047	0.963	0.208	2.3
Wet	LR	0.852 ± 0.011	0.418 ± 0.037	0.777 ± 0.134	0.423 ± 0.113	0.837	0.419	47.7
	ANN	0.946 ± 0.045	0.236 ± 0.099	0.949 ± 0.025	0.217 ± 0.101	0.947	0.232	14.0
	RFR	0.937 ± 0.005	0.272 ± 0.019	0.884 ± 0.044	0.331 ± 0.132	0.926	0.284	15.2
	BTR	0.955 ± 0.005	0.231 ± 0.026	0.864 ± 0.056	0.352 ± 0.126	0.937	0.255	9.3
	KNN	0.876 ± 0.030	0.379 ± 0.052	0.926 ± 0.030	0.257 ± 0.082	0.886	0.355	26.8
	SVM	0.935 ± 0.009	0.277 ± 0.028	0.897 ± 0.027	0.325 ± 0.136	0.927	0.287	15.2
All	LR	0.811 ± 0.006	0.509 ± 0.012	0.769 ± 0.086	0.519 ± 0.043	0.803	0.511	60.4
	ANN	0.953 ± 0.008	0.253 ± 0.020	0.950 ± 0.024	0.241 ± 0.064	0.952	0.251	13.8
	RFR	0.963 ± 0.005	0.225 ± 0.016	0.930 ± 0.021	0.302 ± 0.085	0.956	0.240	7.5
	BTR	0.972 ± 0.002	0.197 ± 0.010	0.911 ± 0.014	0.338 ± 0.078	0.960	0.225	8.1
	KNN	0.923 ± 0.010	0.326 ± 0.028	0.946 ± 0.019	0.263 ± 0.079	0.928	0.313	21.3
	SVM	0.947 ± 0.007	0.270 ± 0.020	0.928 ± 0.024	0.296 ± 0.073	0.943	0.275	21.3

Performance of machine learning models

The performance indicators of six ML models are presented in Table 4. Except for the LR model, all models accurately predict the fc of CSEBs. The effectiveness of the BTR and ANN models in predicting the fc of CSEBs is comparatively good. Although the BTR model performs well when considering the total data, the effectiveness of ANN is the best for predicting both training and test data. The correlation coefficients of the BTR model are 0.973, 0.937 and 0.960 for fc in dry, wet and all conditions respectively. It is closer to unity compared to the other models, except for fc in wet conditions, where the ANN model shows correlation coefficients with R² equal to 0.947. A similar trend was observed for the other performance indicators (RMSE and α_{20} index).

Figure 8 shows the predicted and measured values of fc for each of the six machine learning models in dry, wet and all conditions. The ANN, RFR and BTR models have fewer points outside the 20% error envelope in all conditions. The ANN models had outliers for fc of 1.2%, 14.0% and 13.8% in dry, wet and all conditions respectively. The RFR model had outliers of 2.3%, 15.2% and 7.5%, while the BTR models had outliers of 2.3%, 9.3% and 8.1%. Overall, the RFR model is the best option for predicting fc in both dry and wet conditions.

Sensitive analysis

Artificial neural networks (ANNs) are complex and non-linear models that can sometimes act as black boxes [65]. Previous studies have shown that SHAP (SHapley Additive exPlanations) is a convenient tool for exploring complex machine learning models with different parameters [66,67]. Since ANN performed best on the test data, we used SHAP to interpret the outputs of the ANN model. The key idea of SHAP is to compute the Shapley values for each feature of the sample to be explained, where each value indicates the contribution of the corresponding feature to the prediction. Figure 9(a-c) show the mean SHAP values for the input parameters based on the ANN technique for fc in dry,

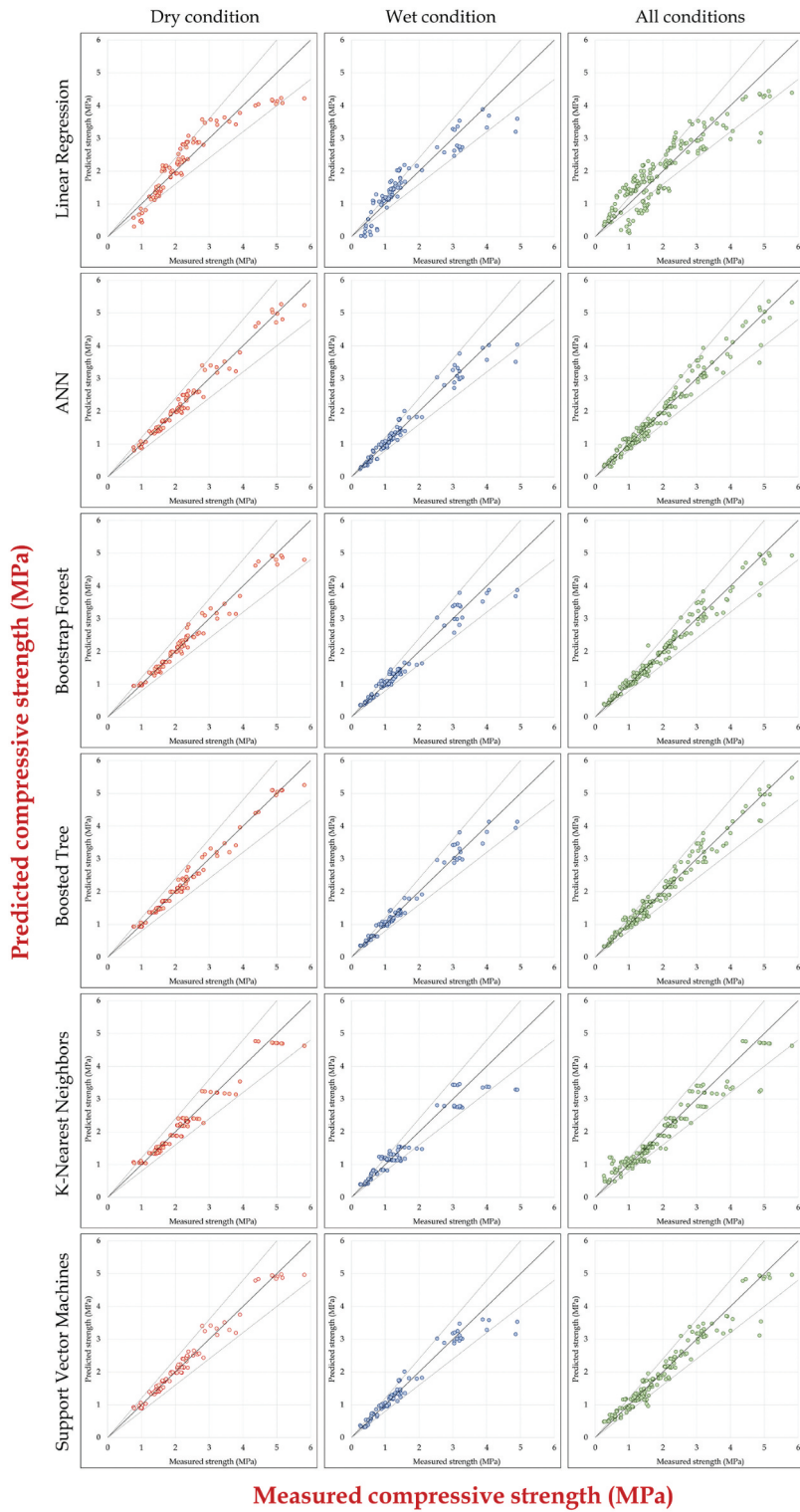


Figure 8. Predicted f_c vs. measured f_c using different ML techniques for dry, wet and all conditions.

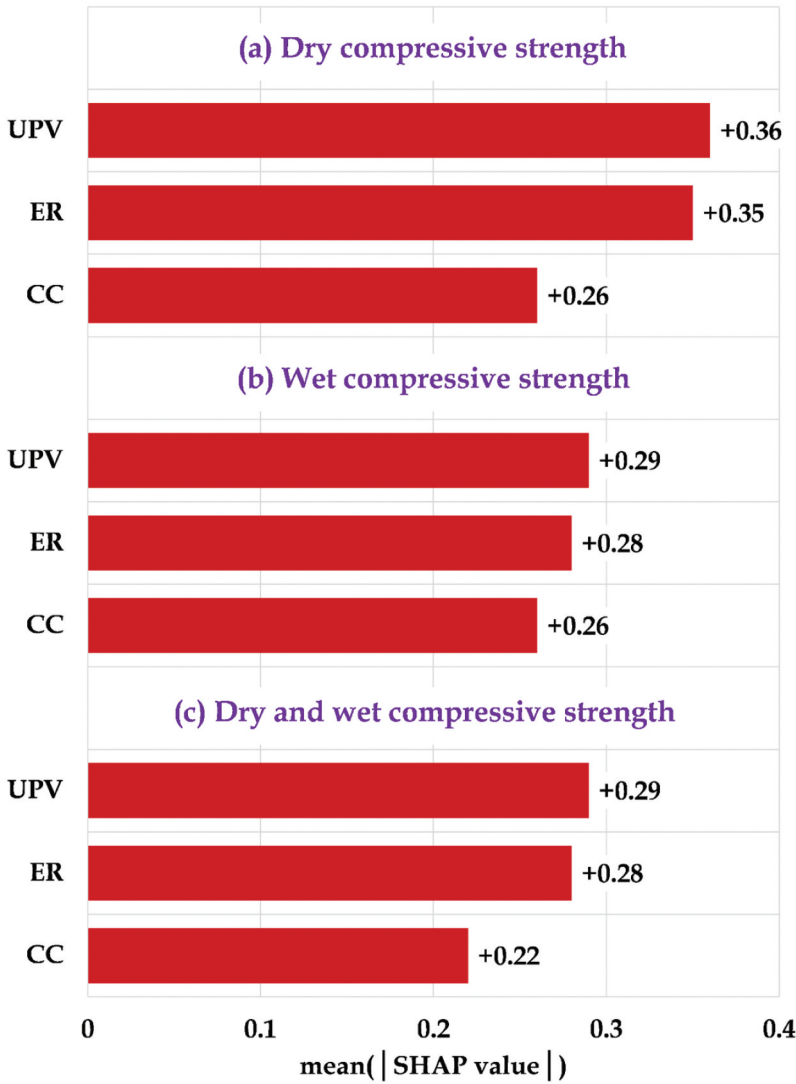


Figure 9. Mean SHAP values using the ANN model.

wet and all conditions respectively. The results show that ultrasonic pulse velocity (UPV) has the highest SHAP value (and thus the most significant influence on the prediction) in all conditions. This means that UPV is the most important factor in predicting f_c . On the other hand, cement content has the lowest SHAP value, meaning that it has relatively less influence on predicting f_c .

The SHAP summary for the prediction of f_c by ANN in dry, wet and all conditions is shown in Figure 10(a-c) respectively. The x-axis shows the SHAP value, which indicates how much the feature influences the predicted result, and the colour illustrates the range of feature values. UPV has a high positive SHAP value of 0.6 in dry conditions, meaning that f_c could be 0.6 MPa higher than the average for higher UPV values. Conversely, UPV has a low negative SHAP value of -0.6 , which means that f_c could be 0.6 MPa lower than the average for lower

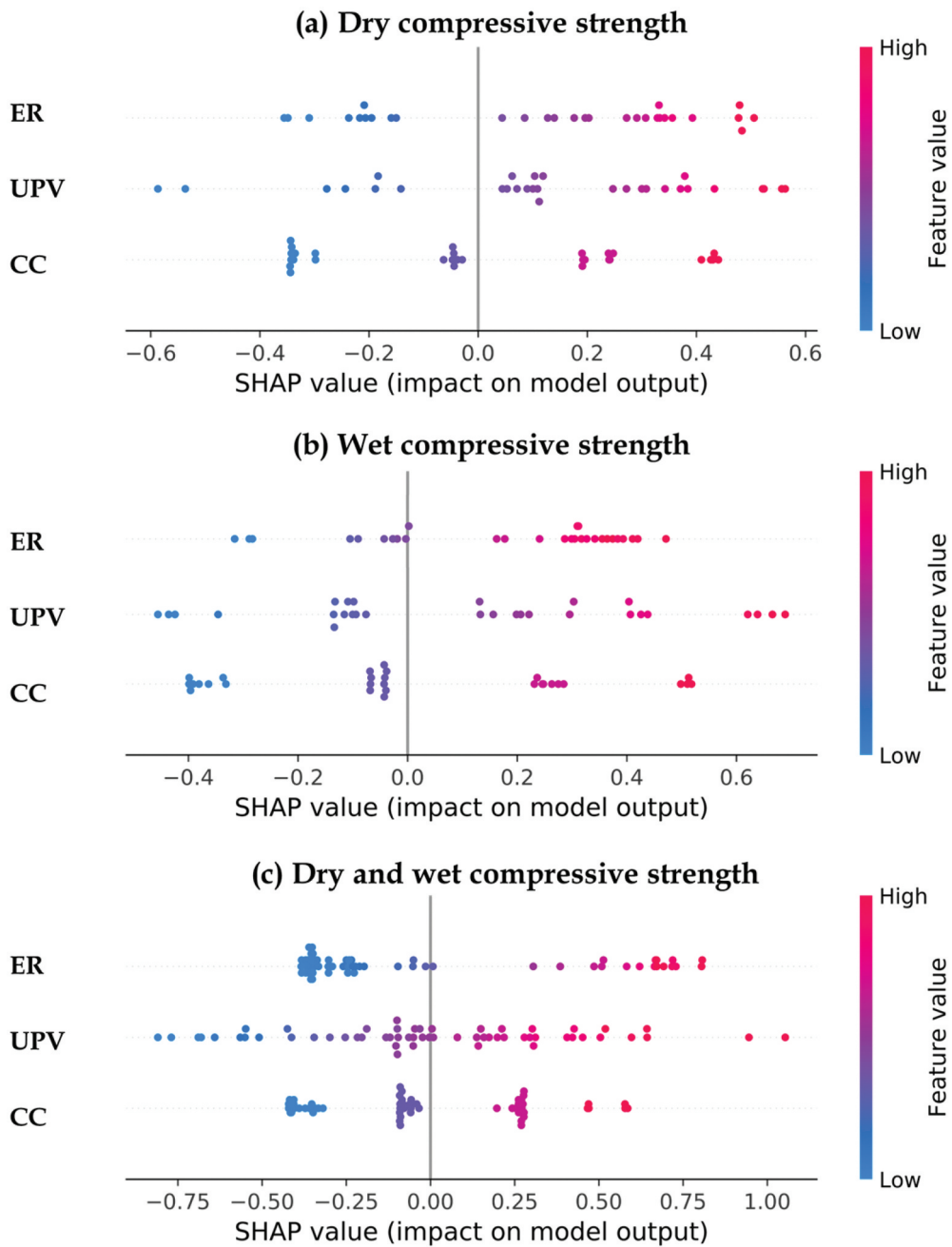


Figure 10. SHAP summary for f_c using ANN.

UPV values. The result of the SHAP value confirms the feature importance analysis in Figure 10, which uses the mean SHAP value. Cement content has the least influence on f_c prediction between UPV and ER. The red dot represents a high feature value. It shows that higher f_c values were observed for higher cement content, UPV and ER. The SHAP analysis shows that using the game theory technique to calculate SHAP could improve the

understanding of the proposed ML techniques and demonstrate that the accuracy of the model's prediction is acceptable.

Comparison of the model with published literature

Figure 11 shows a comparison of predicted and measured compressive strength between the present study and Equation (1), (3), (4) and (5) proposed in the published literature [5,19]. It is worth noting that the use of UPV or ER to predict the compressive strength of CSEBs is rarely found in the published literature. Sathiparan et al. [5] used the same data set and proposed the empirical equation for predicting the compressive strength of CSEBs in air-dry and wet conditions using UPV and ER. Kasinikota and Tripura [19] used UPV to predict the compressive strength of CSEBs in air-dry, oven-dry and wet conditions. The UPV and compressive strength are varied in the range of 0.95–2.14 km/s and 0.73–6.74 MPa, respectively. The equations proposed by both published literatures showed less accuracy compared to the ML model using BDT. The predicted values by the equations proposed by Sathiparan et al. [5] were closer to the measured values, $R^2 = 0.88$ and $RMSE = 0.67$ MPa. The predicted values by equations proposed by Kasinikota and Tripura [6] were mostly overestimated and less close to the

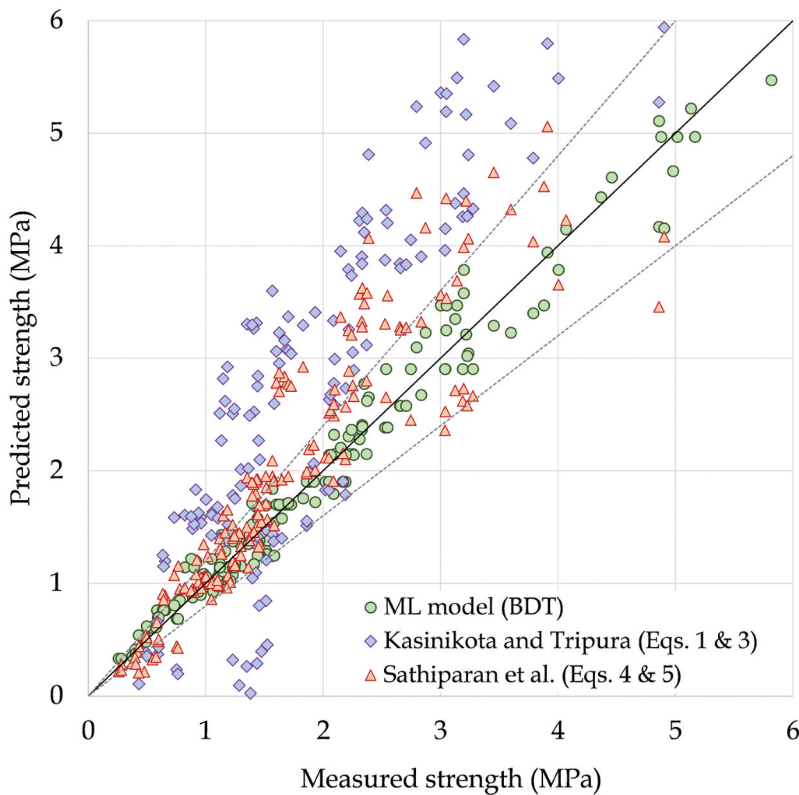


Figure 11. Comparison of performance of ML models and proposed equations by published literature [5,19].

measured value as $R^2 = 0.81$ and $RMSE = 1.30$ MPa. It was shown that the ML model can predict the compressive strength more accurately compared to the empirical equations.

Practical implementation

As masonry, and especially earth masonry, loses strength over time, appropriate care is required to maintain it in good condition. To achieve this, important factors need to be taken into account when selecting a method and materials for repairing the structure. Prior to repair, a number of tests need to be carried out to provide up to date information on the condition of the structure, the compressive strength of the CSEBs and other factors, without compromising serviceability. Non-destructive testing has been shown to be an effective way of obtaining vital details about the quality and uniformity of masonry work without causing damage. Masonry structures can be inspected and assessed using these non-destructive testing techniques without causing any damage to them. This allows masonry structures to be properly maintained and repaired, maintaining their structural integrity and safety. As a result, this work provides a methodical evaluation of the compressive strength prediction of CSEBs using non-destructive testing methods and machine learning techniques. This evaluation can help to expand the knowledge and practical applications of this subject.

Conclusions

The framework for predicting the f_c of CSEBs using NDT measurements and ML models is presented in the present study. 180 experimental specimens (90 data points each for dry and wet conditions) were taken to train and test the models. As basic ML predictors, LR, ANN, BTR, RFR, KNN and SVM were adapted and trained. The following conclusions can be drawn from the results:

- The statistical analysis shows that the use of UPV can be a reliable test to determine the f_c of CSEBs compared to ER.
- ANN, BTR and RFR performed better than other machine learning models tested in this study for predicting f_c .
- Unlike cement content, the results of feature significance analysis using SHAP indicate that UPV and ER are the most important variables affecting the prediction of f_c .

In conclusion, this study provides a comprehensive assessment of the f_c of CSEBs, which could contribute to the existing knowledge and influence the practical application of this field. In addition, the performance of the machine learning model could be improved by adding more data. Therefore, it is necessary to maintain the extensive dataset for mixed parameters, non-destructive measurement and f_c of CSEBs. With the help of accurately predicted model techniques, material scientists and designers could choose the best method to evaluate the field performance of CSEBs.

Abbreviations used in this study

NDT	Non-destructive testing
ANN	Artificial neural network
BTR	Boosted Tree Regression
CC	Cement content
CSEB	Cement stabilised earth block
ER	Electrical resistivity
f_c	Compressive strength
LR	Linear regression
KNN	K-nearest Neighbors
MDD	Maximum dry density
ML	Machine learning
RFR	Random forest regression
RMSE	Root Mean Squared Error
R^2	Coefficient of determination
SHAP	SHapley Additive exPlanations
SVR	Support Vector Regression
UPV	Ultrasonic pulse velocity
W/C	Water-to-cement

Disclosure statement

No potential conflict of interest was reported by the author(s).

ORCID

Pratheeba Jayananthan  <http://orcid.org/0000-0003-0476-3964>

References

- [1] Sundaralingam K, Peiris A, Anburuvel A, et al. Quarry dust as river sand replacement in cement masonry blocks: Effect on mechanical and durability characteristics. *Mater.* 2022;21:101324. doi: 10.1016/j.mtla.2022.101324
- [2] Sathiparan N, Subramaniam DN, Malsara KGN, et al. Thermal comfort analysis of fired-clay brick, cement-sand block and cement stabilized earth block masonry house models. *Innov Infrastruct Solut.* 2022;7(2):147. doi: 10.1007/s41062-022-00744-9
- [3] Yogananth Y, Thanushan K, Sangeeth P, et al. Comparison of strength and durability properties between earth-cement blocks and cement-sand blocks. *Innov Infrastruct Solut.* 2019;4(1):50. doi: 10.1007/s41062-019-0238-8
- [4] Sathiparan N. Mesh type seismic retrofitting for masonry structures: critical issues and possible strategies. *Eur J Environ Civ Eng.* 2015;19(9):1136–1154. doi: 10.1080/19648189.2015.1005160
- [5] Sathiparan N, Jayasundara WGBS, Samarakoon KSD, et al. Prediction of characteristics of cement stabilized earth blocks using non-destructive testing: Ultrasonic pulse velocity and electrical resistivity. *Mater.* 2023;29:101794. doi: 10.1016/j.mtla.2023.101794
- [6] Lombillo I, Villegas L, Fodde E, et al. In situ mechanical investigation of rammed earth: Calibration of minor destructive testing. *Constr Build Mater.* 2014;51:451–460. doi:10.1016/j.conbuildmat.2013.10.090
- [7] Sathiparan N, Anjalee WAV, Kandage KKS. The scale effect on small-scale modelling of cement block masonry. *Mater Struct.* 2016;49(7):2935–2946. doi: 10.1617/s11527-015-0696-1

- [8] Gholizadeh S. A review of non-destructive testing methods of composite materials. *Procedia Struct Integr.* 2016;1:50–57. doi: [10.1016/j.prostr.2016.02.008](https://doi.org/10.1016/j.prostr.2016.02.008)
- [9] Gaydecki P, Fernandes B, Quek S, et al. Inductive and magnetic field inspection systems for rebar visualization and corrosion estimation in reinforced and pre-stressed concrete. *Case Stud NondestrTest Eval.* 2007;22(4):255–298. doi: [10.1080/10589750701362616](https://doi.org/10.1080/10589750701362616)
- [10] Fang Z, Qajar J, Safari K, et al. Application of Non-Destructive Test Results to Estimate Rock Mechanical Characteristics— a Case Study. *Miner.* 2023;13(4):472. doi: [10.3390/min13040472](https://doi.org/10.3390/min13040472)
- [11] Liu L, Miramini S, Hajimohammadi A. Characterising fundamental properties of foam concrete with a non-destructive technique. *Case Stud NondestrTest Eval.* 2019;34(1):54–69. doi: [10.1080/10589759.2018.1525378](https://doi.org/10.1080/10589759.2018.1525378)
- [12] Rashid K, Waqas R. Compressive strength evaluation by non-destructive techniques: An automated approach in construction industry. *J Buil Eng.* 2017;12:147–154. doi: [10.1016/j.jobe.2017.05.010](https://doi.org/10.1016/j.jobe.2017.05.010)
- [13] Ivanchev I. Investigation with non-destructive and destructive methods for assessment of concrete compressive strength. *Appl Sci.* 2022;12(23):12172. doi: [10.3390/app122312172](https://doi.org/10.3390/app122312172)
- [14] Saleh E, Tarawneh A, Dwairi H, et al. Guide to non-destructive concrete strength assessment: Homogeneity tests and sampling plans. *J Buil Eng.* 2022;49:104047. doi: [10.1016/j.jobe.2022.104047](https://doi.org/10.1016/j.jobe.2022.104047)
- [15] Singh N, Singh SP. Evaluating the performance of self compacting concretes made with recycled coarse and fine aggregates using non destructive testing techniques. *Constr Build Mater.* 2018;181:73–84. doi: [10.1016/j.conbuildmat.2018.06.039](https://doi.org/10.1016/j.conbuildmat.2018.06.039)
- [16] Shakr Piro N, Mohammed A, Hamad SM, et al. Electrical resistivity-Compressive strength predictions for normal strength concrete with waste steel slag as a coarse aggregate replacement using various analytical models. *Constr Build Mater.* 2022;327:127008. doi:[10.1016/j.conbuildmat.2022.127008](https://doi.org/10.1016/j.conbuildmat.2022.127008)
- [17] Yılmaz T, Ercikdi B. Predicting the uniaxial compressive strength of cemented paste backfill from ultrasonic pulse velocity test. *Case Stud NondestrTest Eval.* 2016;31(3):247–266. doi: [10.1080/10589759.2015.1111891](https://doi.org/10.1080/10589759.2015.1111891)
- [18] Jiang H, Han J, Li Y, et al. Relationship between ultrasonic pulse velocity and uniaxial compressive strength for cemented paste backfill with alkali-activated slag. *Case Stud Nondestr Test Eval.* 2020;35(4):359–377. doi: [10.1080/10589759.2019.1679140](https://doi.org/10.1080/10589759.2019.1679140)
- [19] Kasinikota P, Tripura DD. Prediction of physical-mechanical properties of hollow interlocking compressed unstabilized and stabilized earth blocks at different moisture conditions using ultrasonic pulse velocity. *J Buil Eng.* 2022;48:103961. doi: [10.1016/j.jobe.2021.103961](https://doi.org/10.1016/j.jobe.2021.103961)
- [20] Ahmad A, Ahmad W, Aslam F, et al. Compressive strength prediction of fly ash-based geopolymer concrete via advanced machine learning techniques. *Case Studies Construction Mater.* 2022;16:e00840. doi: [10.1016/j.cscm.2021.e00840](https://doi.org/10.1016/j.cscm.2021.e00840)
- [21] Zhang LV, Marani A, Nehdi ML. Chemistry-informed machine learning prediction of compressive strength for alkali-activated materials. *Constr Build Mater.* 2022;316:126103. doi: [10.1016/j.conbuildmat.2021.126103](https://doi.org/10.1016/j.conbuildmat.2021.126103)
- [22] Wu J, Jing H, Yin Q, et al. Strength prediction model considering material, ultrasonic and stress of cemented waste rock backfill for recycling gangue. *J Clean Prod.* 2020;276:123189. doi:[10.1016/j.jclepro.2020.123189](https://doi.org/10.1016/j.jclepro.2020.123189)
- [23] Bilgehan M. A comparative study for the concrete compressive strength estimation using neural network and neuro-fuzzy modelling approaches. *Case Stud NondestrTest Eval.* 2011;26(1):35–55. doi: [10.1080/10589751003770100](https://doi.org/10.1080/10589751003770100)
- [24] Vidya Sagar R, Dutta M. Combined usage of acoustic emission technique and ultrasonic pulse velocity test to study crack classification in reinforced concrete structures. *Case Stud NondestrTest Eval.* 2021;36(1):62–96. doi: [10.1080/10589759.2019.1692013](https://doi.org/10.1080/10589759.2019.1692013)
- [25] Asteris PG, Lourenço PB, Hajihassani M, et al. Soft computing-based models for the prediction of masonry compressive strength. *Eng Struct.* 2021;248:113276. doi: [10.1016/j.engstruct.2021.113276](https://doi.org/10.1016/j.engstruct.2021.113276)

- [26] Sharafati A, Haji Seyed Asadollah SB, Al-Ansari N. Application of bagging ensemble model for predicting compressive strength of hollow concrete masonry prism. *Ain Shams Eng J.* 2021;12(4):3521–3530. doi: [10.1016/j.asej.2021.03.028](https://doi.org/10.1016/j.asej.2021.03.028)
- [27] Lan G, Wang Y, Zeng G, et al. Compressive strength of earth block masonry: Estimation based on neural networks and adaptive network-based fuzzy inference system. *Compos Struct.* 2020;235:111731. doi:[10.1016/j.compstruct.2019.111731](https://doi.org/10.1016/j.compstruct.2019.111731)
- [28] Ren Q, Wang G, Li M, et al. Prediction of rock compressive strength using machine learning algorithms based on spectrum analysis of geological hammer. *Geotech Geol Eng.* 2019;37(1):475–489. doi: [10.1007/s10706-018-0624-6](https://doi.org/10.1007/s10706-018-0624-6)
- [29] Aboutaleb S, Behnia M, Bagherpour R, et al. Using non-destructive tests for estimating uniaxial compressive strength and static Young's modulus of carbonate rocks via some modeling techniques. *Bull Eng Geol Environ.* 2018;77(4):1717–1728. doi: [10.1007/s10064-017-1043-2](https://doi.org/10.1007/s10064-017-1043-2)
- [30] Asteris PG, Skentou AD, Bardhan A, et al. Soft computing techniques for the prediction of concrete compressive strength using Non-Destructive tests. *Constr Build Mater.* 2021;303:124450. doi: [10.1016/j.conbuildmat.2021.124450](https://doi.org/10.1016/j.conbuildmat.2021.124450)
- [31] Khashman A, Akpinar P. Non-destructive prediction of concrete compressive strength using neural networks. *Procedia Comput Sci.* 2017;108:2358–2362. doi: [10.1016/j.procs.2017.05.039](https://doi.org/10.1016/j.procs.2017.05.039)
- [32] El-Mir A, El-Zahab S, Sbartaï ZM, et al. Machine learning prediction of concrete compressive strength using rebound hammer test. *J Buil Eng.* 2023;64:105538. doi: [10.1016/j.jobe.2022.105538](https://doi.org/10.1016/j.jobe.2022.105538)
- [33] Li D, Tang Z, Kang Q, et al. Machine learning-based method for predicting compressive strength of concrete. *Processes.* 2023;11(2):390. doi: [10.3390/pr11020390](https://doi.org/10.3390/pr11020390)
- [34] Xin Z, Ke D, Zhang H, et al. Non-destructive evaluating the density and mechanical properties of ancient timber members based on machine learning approach. *Constr Build Mater.* 2022;341:127855. doi:[10.1016/j.conbuildmat.2022.127855](https://doi.org/10.1016/j.conbuildmat.2022.127855)
- [35] Sathiparan N, Jaasim JHM, Banujan B. Sustainable production of cement masonry blocks with the combined use of fly ash and quarry waste. *Mater.* 2022;26:101621. doi: [10.1016/j.mtl.2022.101621](https://doi.org/10.1016/j.mtl.2022.101621)
- [36] Poorveekan K, Ath KMS, Anburuvel A, et al. Investigation of the engineering properties of cementless stabilized earth blocks with alkali-activated eggshell and rice husk ash as a binder. *Constr Build Mater.* 2021;277:122371. doi: [10.1016/j.conbuildmat.2021.122371](https://doi.org/10.1016/j.conbuildmat.2021.122371)
- [37] ASTM-C597. Standard test method for pulse velocity through concrete. West Conshohocken, PA: ASTM International; 2010.
- [38] Carrasco EVM, Silva SR, Mantilla JNR. Assessment of mechanical properties and the influence of the addition of sawdust in soil–cement bricks using the technique of ultrasonic anisotropic inspection. *J Mater Civ Eng.* 2014;26(2):219–225. doi: [10.1061/\(ASCE\)MT.1943-5533.0000723](https://doi.org/10.1061/(ASCE)MT.1943-5533.0000723)
- [39] ASTM-C1876. Standard test method for bulk electrical resistivity or bulk conductivity of concrete. West Conshohocken, PA: ASTM International; 2012.
- [40] Subramaniam DN, Jeyanthan P, Sathiparan N. Soft computing techniques to predict the electrical resistivity of pervious concrete. *Asian J Civ Eng.* 2023; doi: [10.1007/s42107-023-00806-y](https://doi.org/10.1007/s42107-023-00806-y)
- [41] ASTM-C109. Standard test method for compressive strength of hydraulic cement mortars (using 2-in. or [50 mm] cube specimens). West Conshohocken, PA: ASTM International; 2020.
- [42] Ahmed HU, Mohammed AA, Mohammed A, et al. Soft computing models to predict the compressive strength of GGBS/FA- geopolymer concrete. *Plos One.* 2022;17(5):e0265846. doi: [10.1371/journal.pone.0265846](https://doi.org/10.1371/journal.pone.0265846)
- [43] Jeyanthan P. Role of different types of RNA molecules in the severity prediction of SARS-CoV-2 patients. *Pathol Res Pract.* 2023;242:154311. doi: [10.1016/j.prp.2023.154311](https://doi.org/10.1016/j.prp.2023.154311)
- [44] Jeyanthan P. SARS-CoV-2 diagnosis using transcriptome data: A machine learning approach. *SN Comput Sci.* 2023;4(3):218. doi: [10.1007/s42979-023-01703-6](https://doi.org/10.1007/s42979-023-01703-6)

- [45] Lek S, Park YS. Artificial neural networks. In: Jørgensen SE Fath BD, editors. *Encyclopedia of Ecology*. Oxford: Elsevier; 2008. pp. 237–245. doi: [10.1016/B978-008045405-4.00173-7](https://doi.org/10.1016/B978-008045405-4.00173-7).
- [46] Jeyanathan P. Prolonged viral shedding prediction on non-hospitalized, uncomplicated SARS-CoV-2 patients using their transcriptome data, computer methods and programs in biomedicine update. *Comput Methods Programs Biomed*. 2022;2:100070. doi: [10.1016/j.cmpbup.2022.100070](https://doi.org/10.1016/j.cmpbup.2022.100070)
- [47] Sathiparan N, Jeyanathan P, Subramaniam DN. Effect of aggregate size, aggregate to cement ratio and compaction energy on ultrasonic pulse velocity of pervious concrete: prediction by an analytical model and machine learning techniques. *Asian J Civ Eng*. 2023; doi: [10.1007/s42107-023-00790-3](https://doi.org/10.1007/s42107-023-00790-3)
- [48] Lin P, Ding F, Hu G, et al. Machine learning-enabled estimation of crosswind load effect on tall buildings. *J Wind Eng Ind Aerodyn*. 2022;220:104860. doi:[10.1016/j.jweia.2021.104860](https://doi.org/10.1016/j.jweia.2021.104860)
- [49] Sathiparan N, Jeyanathan P. Prediction of masonry prism strength using machine learning technique: Effect of dimension and strength parameters. *Mater Today Commun*. 2023;35:106282. doi: [10.1016/j.mtcomm.2023.106282](https://doi.org/10.1016/j.mtcomm.2023.106282)
- [50] Guillen MD, Aparicio J, Esteve M. Gradient tree boosting and the estimation of production frontiers. *Expert Syst Appl*. 2023;214:119134. doi: [10.1016/j.eswa.2022.119134](https://doi.org/10.1016/j.eswa.2022.119134)
- [51] Elith J, Leathwick JR, Hastie T. A working guide to boosted regression trees. *J Anim Ecol*. 2008;77(4):802–813. doi: [10.1111/j.1365-2656.2008.01390.x](https://doi.org/10.1111/j.1365-2656.2008.01390.x)
- [52] Hu L, Wang H, Qian H, et al. Centrifuge-less dispersive liquid-liquid microextraction base on the solidification of switchable solvent for rapid on-site extraction of four pyrethroid insecticides in water samples. *J Chromatogr A*. 2016;1472:1–9. doi: [10.1016/j.chroma.2016.10.013](https://doi.org/10.1016/j.chroma.2016.10.013)
- [53] Chanal D, Yousfi Steiner N, Petrone R, et al. Online diagnosis of PEM fuel cell by fuzzy C-means clustering. In: Cabeza LF, editor *Encyclopedia of Energy Storage*. Oxford: Elsevier; 2022. pp. 359–393.
- [54] Song Y, Kong X, Zhang C. A large-scale-nearest neighbor classification algorithm based on neighbor relationship preservation. *Wireless Commun Mobile Comput*. 2022;2022:7409171. doi: [10.1155/2022/7409171](https://doi.org/10.1155/2022/7409171)
- [55] Saini I, Singh D, Khosla A. QRS detection using K-Nearest Neighbor algorithm (KNN) and evaluation on standard ECG databases. *J Adv Res*. 2013;4(4):331–344. doi: [10.1016/j.jare.2012.05.007](https://doi.org/10.1016/j.jare.2012.05.007)
- [56] Xia Y. Chapter eleven - correlation and association analyses in microbiome study integrating multiomics in health and disease. In: Sun J, editor. *Progress in Molecular Biology and Translational Science*, Academic Press. 2020. pp. 309–491. [10.1016/bs.pmbts.2020.04.003](https://doi.org/10.1016/bs.pmbts.2020.04.003)
- [57] Chen Y-P-P, Ivanova EP, Wang F, et al. 9.15 - Bioinformatics. In: Liu H-W Mander L, editors. *Comprehensive Natural Products II*. Oxford: Elsevier; 2010. pp. 569–593. doi: [10.1016/B978-008045382-8.00729-2](https://doi.org/10.1016/B978-008045382-8.00729-2).
- [58] Sun W, Chang C, Long Q, Bayesian non-linear support vector machine for high-dimensional data with incorporation of graph information on features, *Proc IEEE Int Conf Big Data 2019; Los Angeles, CA*; 2019. p. 4874–4882.
- [59] An W, Liang M. Fuzzy support vector machine based on within-class scatter for classification problems with outliers or noises. *Neuro comput*. 2013;110:101–110. doi: [10.1016/j.neucom.2012.11.023](https://doi.org/10.1016/j.neucom.2012.11.023)
- [60] Ndagi A, Umar AA, Hejazi F, et al. Non-destructive assessment of concrete deterioration by ultrasonic pulse velocity: A review. *IOP Conference Series: Earth And Environ Sci*. 2019;357(1):012015. doi: [10.1088/1755-1315/357/1/012015](https://doi.org/10.1088/1755-1315/357/1/012015)
- [61] Sathiparan N, Anburuvel A, Maduwanthi KAPN, et al. Effect of moisture condition on cement masonry blocks with different fine aggregates: river sand, lateritic soil and manufactured sand. *Sādhanā*. 2022;47(4):270. doi: [10.1007/s12046-022-02054-3](https://doi.org/10.1007/s12046-022-02054-3)
- [62] Zhou M, Wang J, Cai L, et al. Laboratory investigations on factors affecting soil electrical resistivity and the measurement. *IEEE Trans Sustain Energy*. 2015;51(6):5358–5365. doi: [10.1109/TIA.2015.2465931](https://doi.org/10.1109/TIA.2015.2465931)

- [63] Cao Z, Xiang L, Peng E, et al. Experimental Study on Electrical Resistivity of Cement-Stabilized Lead-Contaminated Soils. *Adv Civ Eng* 2018. 2018;2018:1–11. doi: [10.1155/2018/4628784](https://doi.org/10.1155/2018/4628784)
- [64] Kibria G, Hossain MS. Investigation of geotechnical parameters affecting electrical resistivity of compacted clays. *J Geotech Geoenviron Eng*. 2012;138(12):1520–1529. doi: [10.1061/\(ASCE\)GT.1943-5606.0000722](https://doi.org/10.1061/(ASCE)GT.1943-5606.0000722)
- [65] Shah SFA, Chen B, Zahid M, et al. Compressive strength prediction of one-part alkali activated material enabled by interpretable machine learning. *Constr Build Mater*. 2022;360:129534. doi: [10.1016/j.conbuildmat.2022.129534](https://doi.org/10.1016/j.conbuildmat.2022.129534)
- [66] Zhang J, Niu W, Yang Y, et al. Machine learning prediction models for compressive strength of calcined sludge-cement composites. *Constr Build Mater*. 2022;346:128442. doi:[10.1016/j.conbuildmat.2022.128442](https://doi.org/10.1016/j.conbuildmat.2022.128442)
- [67] Quan Tran V, Quoc Dang V, Si Ho L. Evaluating compressive strength of concrete made with recycled concrete aggregates using machine learning approach. *Constr Build Mater*. 2022;323:126578. doi: [10.1016/j.conbuildmat.2022.126578](https://doi.org/10.1016/j.conbuildmat.2022.126578)